polarization in a 2.5 T magnetic field. Even higher deuteron polarizations have been achieved in materials doped by new trityl free radicals [46], in irradiated deuterated butanol [46, 47], and in irradiated deuterated ammonia [48]. Common to these and to irradiated ^{6}LiD is a narrow "Electron Spin Resonance" (ESR) line that allows one to reach a low deuteron spin temperature by dynamic cooling of the spin–spin interactions of the unpaired electrons, as had been predicted in earlier studies by the PT team at CERN [49].

For the large targets an axial field geometry was required, with a field uniformity in the range of 10^{-5}. Superconducting solenoid magnets were designed with improved coil winding techniques, using rectangular wire to reduce the number of compensation and trimming coils. The rectangular wire fabrication technique was developed in collaboration with industry. The technology for achieving a uniform field in superconducting solenoids has found other applications, including magnetic resonance imaging (MRI).

While this highlight focused on technical development at CERN, clearly other laboratories also contributed to the field and CERN profited from exchanges with them. This development has now enabled us to reach over 90% polarization, positive and negative, of almost any nuclear spin. Targets can be operated in frozen spin mode in a relatively low field of any orientation, and in DNP mode for high intensity beams. Beyond experiments in nuclear and particle physics, applications of DNP are emerging in macromolecular chemistry and in MRI.

5.9 The Silicon Age: Micrometre Precision Millions of Times a Second

Erik Heijne

Silicon sensors and custom-designed integrated circuits ("chips") are essential components in today's particle physics experiments. These silicon devices replaced earlier tracking instruments such as spark chambers and bubble chambers which recorded the particle trajectories photographically. While gaseous wire chambers remain preferred for covering large surfaces [Highlight 4.8], they are no longer competitive in spatial resolution and signal speed for the smaller areas close to the interaction region. The characteristic features that contributed to the breakthrough of silicon (Si) detectors between 1980 and 2000 were: (i) the small, stable and well-defined dimensions of the sensor cells of typically around 100 μm; (ii) the potential to resolve several particles, incident simultaneously on mm-size area; (iii) the short signals of less than 20 nanoseconds (ns); and (iv) the progressive miniaturization of the associated electronics for the processing of the particle signals: by 2010, 65 000 signal amplifiers, digitizers and memory could be

placed on a single substrate of Si (15 mm × 15 mm), a miniaturization which was, and continues to be, driven by industry. The introduction of Si devices designed for multiple particle detection was spearheaded by scientists at CERN who exploited the advances in microelectronics technology. Si microstrip detectors were soon widely adopted in experiments that studied short-lived charm and beauty particles. Their decay-path, less than about a mm, could now be distinguished separately from traces that originate from the primary interaction vertex. Early steps in this innovation are illustrated here.

Semiconductor materials such as Si, germanium (Ge) or diamond (C) contain only few free charge carriers, contrary to metals in which a large density of free electrons easily allows an electrical current to flow. Nevertheless, a small current signal can be generated in a semiconductor by the passage of a fast, charged particle, which loses some of its energy and liberates charges. An electric field is applied between metallic contacts (Fig. 5.21) under which the charges drift to the electrodes and induce a signal, which is sensed by a connected amplifier. In Si it is necessary to provide rectifying contacts (the p+ contact in Fig. 5.21) in order to prevent a 'leakage current' which would obscure these small signal currents. Such a structure is called a 'diode', and technology has been developed to imprint a large matrix, e.g. 256 × 256 of adjacent diodes on the same Si substrate. In most cases, the particle generates signal currents simultaneously in two or more sensor cells and, by interpolation, it is possible to determine its position in space with a few μm precision, considerably smaller than the dimension of the sensor cell itself.

A complete reconstruction of the trajectory of a particle requires the measurement of several points in space and 'telescopic' arrangements of three to four successive Si detector planes usually surround the interaction region in an experiment.

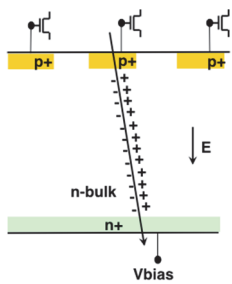

Fig. 5.21. Schematic drawing of a segmented Si detector, with an incident ionizing particle. Segmented, rectifying contacts p+ are made by ion-implantation of boron, the continuous n+ contact is made by implantation of phosphorous or arsenic ions. A biasing voltage Vbias is applied across the detector, generating an electrical field E throughout the n-type bulk Si, which separates the charges created by an incident particle. The resulting signal current is sensed by the amplifiers connected to the rectifying contacts (Drawing not to scale).

In 1980 vertex reconstruction was achieved for the first time using a Si microstrip detector [50], in collaboration with the NA11 experiment at the SPS, using the setup shown in Fig. 5.22. This detector was a one-dimensional matrix of 100 metal-Si diodes, 200 μm wide gold-evaporated bands on a 20 mm × 30 mm Si substrate. The design was inspired by the earlier, so-called 'Si checker-board' segmented detectors used in the 'BOL' experiment [51] at the Nuclear Physics Institute IKO in Amsterdam, operating at their cyclotron since 1967. This IKO device had perpendicular segmentation at the front and back, hence providing 2-dimensional particle positions, while the CERN detectors had strips only on one side, and several planes were required for 3-dimensional spatial coordinates. Soon thereafter, the MPI/TU Munich and CERN collaboration perfected the exploitation of Si microstrip detectors for charm physics research. In parallel, experiment WA75 using the Omega spectrometer [Highlight 3.7] also adopted Si microstrip detectors to determine the decay point of charm and beauty particles in an upstream plate of sensitive emulsion. WA75 published the first direct observation of beauty particles decaying into charmed particles in 1985 [52].

Research into new phenomena in elementary particle physics experiments frequently needs increased energy, typically producing more particles in an interaction. However, the new phenomena tend to occur more rarely than the already known processes, so higher beam intensities and interaction rates are required, motivating development of innovative instrumentation. In Si detectors high signal rates (well over 40 MHz) can be handled, as the freed electrons move at speeds of greater than 10000 km/h: the electrical charge in a 0.3 mm thick Si

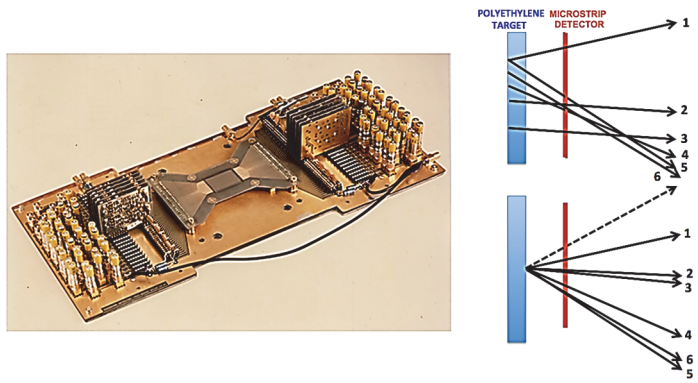

Fig. 5.22. Left: the first operational setup of a segmented, 100-element Si microstrip detector (the rectangle in the centre of the photo), on a support containing a few of the readout amplifier cards. Right: (top) reconstruction of an interaction using only the wire chamber information; (bottom) vertex reconstruction after including the signals from the Si microstrip detector. An additional particle is found as well, the broken line. (Courtesy NA11).

layer can be collected in less than 20 ns. Immediately afterwards, the diode detector is ready for recording another particle. Several particles can be measured simultaneously, even if they are as close as 0.5 mm. For these event topologies, a true 2-dimensional matrix of sensor cells is preferable to combinations of 1-dimensional microstrip detectors. In 1989 it became possible, with the help of the microelectronics team at the EPFL, to produce a first 9 × 12 matrix of a so-called Si pixel detector. In this case a 2-D Si sensor matrix is connected pixel by pixel to a corresponding matrix of readout cells on an integrated circuit, made in CMOS (Complementary Metal-Oxide Silicon) microelectronics technology. Each of these cells comprises a full signal processing circuit with amplifier and digitizer. In recent implementations a memory in each cell can even store the time of incidence and amplitude of a signal from one or several successive particles. In 1992 the second iteration of the Si pixel detector could resolve hundreds of particle tracks on a 6 × 6 cm^2 area and was successfully used for WA94, an ion experiment in the Omega spectrometer. This demonstration helped to dispel much of the prevailing scepticism surrounding the practicality of pixel detectors. Figure 5.23, left shows the two half planes that together constituted one of the seven arrays of the Si pixel telescope. A reconstruction of an ion-event using this instrument in WA97, the successor to WA94, is shown in Fig. 5.23, right.

With the introduction of segmented Si microstrip and pixel detectors, the number of sensing elements in the experiments increased to tens of thousands or

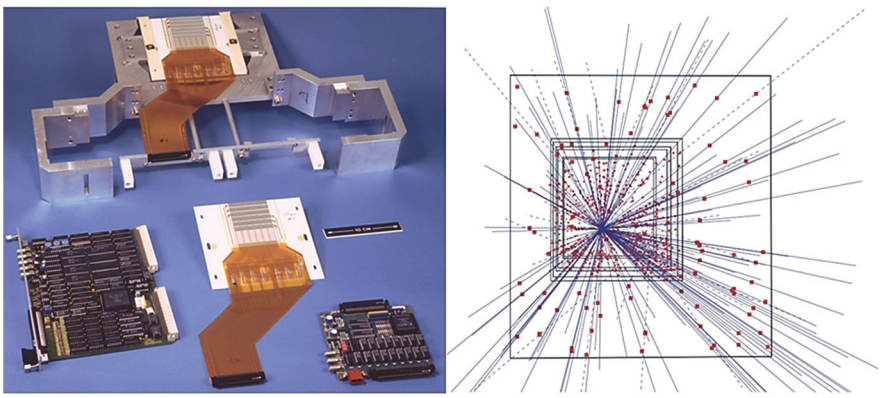

Fig. 5.23. Left: two half-planes from the first CERN silicon pixel telescope for the WA94 Omega spectrometer ion experiment. When mounted together, face-to-face, the six horizontal Si ladders on one, white ceramic support cover the spaces between those on the other support. Also shown are the receiver board (left) and the driver module placed directly near the telescope. Right: reconstruction of tracks from an interacting ion in the WA97 experiment, using the pixel telescope with 7 double planes (Source: WA97).

even hundreds of millions. It is obvious that miniaturized, integrated electronic circuits are required for the processing of such a multitude of signals. From 1985 onward, a Si integrated circuit design expertise was established at CERN, with the 16-channel AMPLEX chip as the first outcome, used in the UA2 Si pad detector [Highlight 6.6]. Intensive contacts with experienced groups in universities such as the EPFL in Lausanne and IMEC in Leuven helped to achieve a professional level in chip design. The custom-designed circuits were then manufactured by CMOS chip processing industry, while evaluation and testing proceeded at CERN. Other particle physics institutes soon participated in concerted developments of Si circuits and detector systems. The early steps in the development of the Si pixel detectors have been described in [53, 54]. More recent achievements on electronic circuits and the development of their radiation resistance are reported elsewhere [Highlights 8.6 and 8.7]. The use of silicon detectors in particle physics experiments as well as in space-borne research has grown exponentially over three decades, as illustrated in Fig. 5.24, showing the Si detector area in an experiment as a function of the year of its first operation.

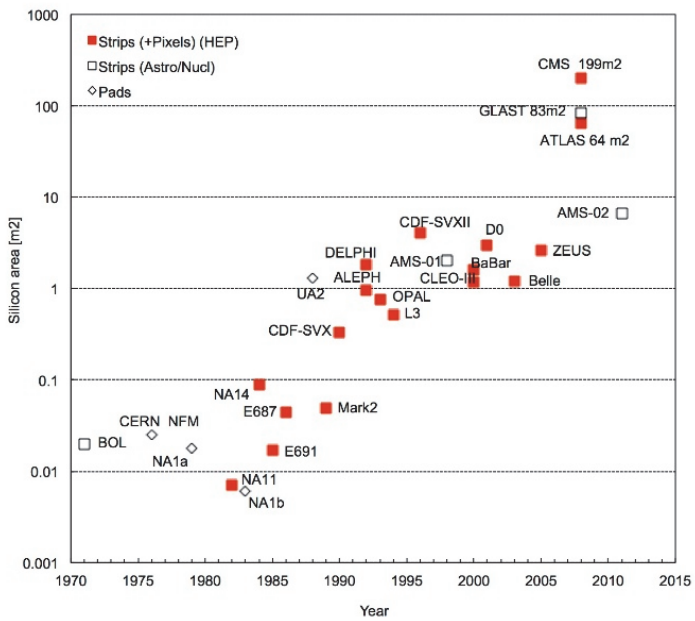

Fig. 5.24. Evolution over time of the surface area of silicon detector systems in particle physics and in recent space-based experiments (Courtesy Y. Unno, KEK).

References

1. D. Pestre, The difficult decision, taken in the 1960s, to construct a 3-400 GeV synchrotron in Europe, in *History of CERN*, Vol. III, ed. J. Kriege (Elsevier, 1996) p. 65.
2. J.B. Adams and E.J.N. Wilson (eds.), *Design Studies for a Large Proton Synchrotron and its Laboratory*, CERN-1970-006 (CERN, Geneva, 1970). http://dx.doi.org/10.5170/CERN-1970-006.
3. J.B. Adams, The CERN 400 GeV Proton Synchrotron (CERN SPS), *Proc. 10th Int. Conf. on High-Energy Accelerators*, *vol. 1*, Protvino, USSR (1977) p. 17.
4. M. Goldsmith and E. Shaw, *Europe's Giant Accelerator*, (Taylor & Francis, London, 1977).
5. Y. Baconnier, P.E. Faugeras, K.H. Kissler, B. de Raad and W. Scandale, Extraction from the CERN SPS, *Proc. 7th Part. Accel. Conf.*, Chicago, USA (1977) p. 1434.
6. R.L. Keizer, L. Reinder, K.H. Kissler and L.R. Oberli, Improvement of the extraction channels of the CERN-SPS accelerator, *IEEE Part. Accel. Conf.*, Washington D.C., USA (1987) p. 1836.
7. Y. Baconnier *et al*., Septum magnets for the extraction channels of the 400 GeV SPS, *6th Int. Conf. on Magnet Technology,* Bratislava, Slovakia (1977) p. 504.
8. W. Schnell, A wide-band travelling-wave accelerating method for a 300 GeV proton synchrotron, *5th Int. Conf. on High-Energy Accelerators*, Frascati, Italy (1965) p. 38.
9. K. Cornelis and R. Schmidt, Commissioning of the SPS as LEP injector, *Proc. 1st European Part. Accel. Conf. (EPAC),* Rome, Italy, (1988) p. 329.
10. M. Benedikt, P. Collier, V. Mertens, J. Poole, K. Schindl (eds.), *LHC Design Report*, *v. 3*, *The LHC Injector Chain*, CERN-2004-003 (CERN, Geneva, 2004). http://dxdoi.org/10.5170/CERN-2004-003-V-3.
11. ECFA 300 GeV Working Group: Volume I - Status Reports of the Working Parties, July 1972; Volume II - Proceedings of the Second Tirrenia Study Week, September 1972; Volume III - Final report of the Executive Committee, CERN/ECFA/72/4 (1973).
12. J.R. Ellis *et al*. (eds.) CERN: the second 25 years, *Phys. Rep.* **403-404** (2004) pp. 1-504.
13. M. Fidecaro, Polarization experiments at the SPS, *Proc. AIP Conf.* **35** (1976) pp. 158-160.
14. F. Dydak, Neutrino Physics, in [12] pp. 57-67.
15. R. Voss, Deep inelastic scattering with muons, in [12] pp. 3-18.
16. B. French, E. Quercigh, Physics with hadron and photon beams at the SPS, in [12] pp. 69-90.
17. C. Lourenco, H.K. Worhi, Heavy flavour hadro-production from fixed-target to collider energies, *Phys. Rep.* **433** 127-180 (2006) hep-ph/0609101.
18. E. Quercigh, K. Safarik, Ion physics at the SPS: the experimental challenge in [12] pp. 51-56.
19. H. Wahl, First observation and precision measurement of direct CP violation: the experiments NA31 and NA48, in [12] pp. 19-25.
20. H. Burkhardt *et al*., The beam and detector for a high-precision measurement of CP violation in neutral kaon decays, *Nucl. Instr. & Meth. A* **268**, 116-143 (1988).
21. H. Burkhardt *et al*., First evidence for direct CP violation, *Phys. Let. B* **206**, 169-176 (1988).
22. M.C. Crowley-Milling (ed.), *The Design of the Control System for the SPS*, CERN-1975-020 (CERN, Geneva, 1975). http://dx.doi.org/0.5170/CERN-1975-020.
23. M.C. Crowley-Milling (ed.), *Experience with the Control System for the SPS*, CERN-1978-009 (CERN, Geneva, 1978). http://dx.doi.org/10.5170/CERN-1978-009.
24. M.C. Crowley-Milling and G.C. Shering (eds.), *The NODAL System for the SPS*, CERN-1978-007 (CERN, Geneva, 1978). http://dx.doi.org/10.5170/CERN-1978-007.

25. F. Beck and B. Stumpe (eds.), *Two Devices for Operator Interaction in the Control of the New CERN 300 GeV Accelerator*, CERN-1973-006. (CERN, Geneva, 1973). http://dx.doi.org/10.5170/CERN-1973-006.
26. E.A. Johnson, Touch display – a novel input/output device for computers, *Electronics Letters* **1**(8), 219 (1965); https://dx.doi.org/10.1049%2Fel%3A19650200.
27. B. Stumpe and C. Sutton, The first capacitive touchscreens at CERN, *CERN Courier* **50** 3 (2010); http://cds.cern.ch/record/1734498.
28. N. Doble *et al.*, The upgraded muon beam at the SPS, *Nucl. Instr. & Meth. A* **343**, 351-362 (1994).
29. G. Mallot *et al*., The COMPASS experiment at CERN, *Nucl. Instr. & Meth. A* **577**, 455-518 (2007) and *Report CERN-PH-EP-2007-001*, arXiv:hep-ex/0703049.
30. V. Fanti *et al*., The beam and detector for the NA48 neutral kaon CP violation experiment at CERN, *Nucl. Instr. & Meth. A* **574**, 433-471 (2007).
31. N. Doble, L. Gatignon and P. Grafstroem, A novel application of bent crystal channelling to the production of simultaneous particle beams, *Nucl. Instr. & Meth. B* **119**, 181-191 (1996).
32. J.R. Batley *et al*., A precision measurement of direct CP violation in the decay of neutral kaons into two pions, *Phys. Lett. B* **544**, 97-112 (2002).
33. J.R. Batley *et al*., Search for direct CP violating charge asymmetries in $K^{\pm}\rightarrow\pi^{\pm}\pi^{+}\pi^{-}$ and $K^{\pm}\rightarrow\pi^{\pm}\pi^{0}\pi^{0}$ decays, *Eur. Phys. J. C* **52**, 875-891 (2007).
34. G.D. Barr *et al.*, Performance of an electromagnetic liquid krypton calorimeter based on a ribbon electrode tower structure, *Nucl. Instr. & Meth. A* **370**, 413-424 (1996).
35. H. Wenninger, In the tracks of the bubble chamber, *CERN Courier*, July 2004 (2004), G.G. Harigel, Bubble chambers, technology and impact on high energy physics; http://www.bo.infn.it/antares/bolle-libro/harigel.pdf.
36. D. Haidt, H. Leutz and H. Wenninger, Optimization of size and shape of a track sensitive H_2/D_2 target for neutrino interactions in BEBC, *Proc. 5th Int. Conf. on Instrumentation for High Energy Physics*, Frascati, Italy (1973) pp. 71-78.
37. P.C. Bosetti *et al*., Analysis of Nucleon Structure Functions in CERN Bubble Chamber Neutrino Experiments, *Nucl. Phys. B* **142**, 1-28 (1978).
38. M. Borghini, Spin temperature model of DNP, *Phys. Rev. Lett.* **20**, 419 (1968).
39. W. de Boer, M. Borghini, K. Morimoto, T.O. Niinikoski and F. Udo, Dynamic polarization of protons, deuterons and carbon-l3 nuclei: thermal contact between nuclear spins and electron spin-spin interaction reservoir, *J. Low Temp. Phys.* **15**, 249 (1974).
40. T. Niinikoski and F. Udo, "Frozen spin" polarized target, *Nucl. Instr. & Meth* **134**, 219 (1976).
41. T. Niinikoski, Dilution Refrigeration: New Concepts, p. 102 in *Proc. 6th Int. Cryo. Eng. Conf., Grenoble 1976*, Ed. K. Mendelssohn (IPC Science and Technology Press, Guilford 1976).
42. R. Bernard *et al*., A Frozen Spin Target with Three Orthogonal Polarization Directions, *Nucl. Instr. & Meth. A* **249**, 176 (1986).
43. T. Niinikoski, Viscometric Study of Binary Mixtures of Butanol and Pentanol with Water and Pinacol, in *Proc. of the 2nd Workshop on Polarized Target Materials*, eds. G. R. Court, S. F. J. Cox, D. A. Cragg and T. O. Niinikoski (SRC, Rutherford Laboratory, 1980).
44. T. Niinikoski and J.-M. Rieubland, Dynamic nuclear polarization in irradiated ammonia below 0.5 K, *Phys. Lett. A* **72**, 141 (1979).

45. D. Adams *et al*., A New Measurement of the spin-dependent structure function $g_1(x)$ of the Deuteron, *Phys. Lett. B* **357**, 248 (1995), and
D. Adams *et al*., The polarized double-cell target of the SMC, *Nucl. Instr. & Meth. A* **437**, 23 (1999).
46. S.T. Goertz *et al*., Highest polarizations in deuterated compounds, *Nucl. Instr. & Meth. A* **526**, 43 (2004).
47. D.G. Crabb, Polarization in radiation-doped butanol and CD_2, *Nucl. Instr. & Meth. A* **526**, 56 (2004).
48. J. Heckmann *et al*., Electron spin resonance and its implication on the maximum nuclear polarization of deuterated solid target materials, *Phys. Rev. B* **74** , 134418 (2006).
49. M. Borghini (ed.), *Choice of Materials for Polarized Proton Targets*, CERN-1966-003 (CERN, Geneva, 1966). http://dx.doi.org/10.5170/CERN-1966-003.
50. E.H.M. Heijne *et al*., A silicon surface barrier microstrip detector designed for high energy physics, Nucl. Instr. & Meth. **178**, pp. 331-343, (1980).
51. L.A.C. Koerts *et al.*, The 'BOL' nuclear research project, *Nucl. Instr. & Meth.* **92**, 157-160 (1971).
52. J.P. Albanese *et al*., Direct observation of the decay of beauty particles into charm particles, *Phys. Lett. B* **158**, 186-192 (1985).
53. F. Anghinolfi *et al*., A 1006 element hybrid silicon pixel detector with strobed binary output, *IEEE Trans. Nucl. Sci.* **NS-39**, 654-661 (1992).
54. E.H.M. Heijne, Semiconductor micropattern pixel detectors: a review of the beginnings, *Nucl. Instr. & Meth. A* **465**, 1-26 (2001).